Heliyon 9 (2023) e13051

Contents lists available at ScienceDirect

Heliyon

journal homepage: www.cell.com/heliyon

Research article

An intelligent planning method to optimize high-density residential layouts considering the influence of wind environments

Xiaoyu Ying [a], Xiaoying Qin [a,b], Liying Shen [a,b], Chunyang Yu [c], Jia Zhang [d,*]

[a] Department of Architecture, Hangzhou City University, Hangzhou, 310015, PR China
[b] College of Civil Engineering and Architecture, Zhejiang University, Hangzhou, 310058, PR China
[c] Department of Industrial Design, Hangzhou City University, Hangzhou, 310015, PR China
[d] Department of Environment Design, Hangzhou City University, Hangzhou, 310015, PR China

ARTICLE INFO

Keywords:
High-density residential layout
Outdoor wind environment
Automatic generation
Fast predict
Optimal solution set

ABSTRACT

There is a growing conflict between building density and the comfort of the external environment in residential construction, especially in high-density cities in China. To address this conflict, a sensible building layout has to take both aspects into account. However, it is difficult for traditional planning approaches to produce a sensible building layout. This is partly due to the fact that an architect's subjective experiences are unreliable. On the other hand, the wind environment simulations of professional software are often time-consuming so that they are difficult to apply efficiently in practice. This study therefore focuses on the automatic generation of optimized high-density residential building layouts as well as the fast and accurate calculation of the corresponding wind environments. By combining the automatic optimization function of a genetic algorithm and the prediction function of a fully convolutional neural network, an intelligent planning method is proposed for producing optimal high-density residential building layouts in consideration of the local wind environment. To further verify its practicality and significance, a case study was carried out in the Yangtze River Delta region, China, through the automatic generation of a residential building layout, wind environment simulation, and a scheme comparison for optimization.

1. Introduction

With the fast growth of high-rise buildings and the dramatic scale of urbanization especially in China, the urban static or strong wind zones have significantly increased in dense countries. This subsequently affects airflow patterns and the comfort of pedestrian-grade wind around the buildings. The urban static or strong wind zone is closely associated with the urban wind environment. A good wind environment will diffuse traffic pollutants, accelerate natural ventilation, and provide comfort to pedestrians. On the other hand, a bad one may hinder the urban ventilation or multiply local wind speeds, thus causing safety issues [1].

Generally, there are two dominant elements that affect the formation of wind environments in urban areas: the buildings' form and urban layout. More specifically, these factors can be described by the height of the buildings [2,3], the plan form of the building complex [4], the orientations of building blocks [5,6], the height differences between buildings [7], the height-to-width ratios of the

* Corresponding author.
E-mail address: zhangjia@zucc.edu.cn (J. Zhang).

https://doi.org/10.1016/j.heliyon.2023.e13051
Received 7 February 2022; Received in revised form 10 December 2022; Accepted 13 January 2023
Available online 20 January 2023

streets [8], the building density [9], etc. These factors become essential in the planning of residential building layouts for an optimized residential wind environment. In the conceptual design stage, it is necessary to simulate the wind environment for each layout scheme in order to identify successful ones. Based on this, the effectiveness of the residential building layouts can be improved to address a suitable wind environment.

Traditional strategies for the study of wind environment focus on field measurements and wind tunnel tests. With the development of computational fluid dynamics (CFD) theory [10] and computer numerical simulation technology [11], CFD software such as FLUENT or PHOENICS [12] are widely used to simulate residential wind environment because of their high reliability. Compared to higher cost and more accurate wind tunnel technologies such as Laser Doppler Anemometry (LDA), Particle Image Velocimetry (PIV), and Large Eddy Simulation (LES), faster and cheaper computer simulation methods are increasingly demanded as long as the margin of error is acceptable [13,14].

However, CFD software currently have some shortages that limits its applications in the planning of residential building layouts. Firstly, it is time-consuming, as a single simulation typically costs at least 20–30 min, and may be 3 to 4 times longer for multiple simulations of multiple schemes. Secondly, the most critical point is that it lacks the mechanism for automatic optimization. The software only presents the simulation data in graphs without any decision-making process about how to optimize. This means that the optimization process relies almost entirely on the architects' own experience. The architects need to iteratively revise the plan and rerun the simulation until successful solutions are developed. But the final scheme may not be the optimal one.

To address these problems, this study proposes an intelligent method for planning of building layouts for residential areas. It uses deep learning technologies imitating the planning process of architects. The innovation is mainly reflected in two aspects. Firstly, it uses a genetic algorithm to automatically generate all types of residential building layout plans, which improves the limitation of architects' personal experience. Secondly, a fully convolutional neural network is applied to simulate the wind environment of all types of residential building layout solutions in a manner of efficiency and effectiveness. As a result, it is possible to select a group of layout schemes with satisfied wind environment all at once, which greatly saves the effort spent on the planning work.

It is organized as follows. In Section 2, the related work is reviewed. A proposed intelligent planning method framework and key operations are detailed in Section 3. Section 4 is a case study to validate the proposed method. Finally, values and limitations are summarized in Sections 5.

2. Related work

2.1. Wind environment

To date, there are two major types of urban architectural studies that consider comfortable wind environments: studies of architectural parameters, and comparative analyses of architectural layout schemes. The former category focuses on the parameter configuration for a single building or group of buildings, such as building coverage, building spacing, building height, building form, and building windward surface. Blocken et al. concluded that the horizontal wind speed at the height of pedestrians increases significantly with the rising of the spacing between parallel buildings [15]. Kubota et al. found that the average wind speed ratio decreased remarkably with the increase of the total building coverage through studying 22 residential areas in Japan [9]. Based on these, Tsang et al. found that the natural ventilation at the pedestrian horizontal height suffered from a reduction if the spacing between the buildings is less than half of the building width. Meanwhile, building podiums can also decrease the natural ventilation around buildings [16]. Tse et al. studied the wind environment of 9 building models at different heights and distances and found that the building spacing matters more than the building height in wind conditions [17].

To further explore the impact of building heights on the wind environment, Ying et al. studied the relations between the floor area ratio, building height, and the outdoor wind environment, concluding that the higher the building, the larger the outdoor comfortable wind area of pedestrian [3]. Adamek et al. studied the building wind environment in Toronto's financial district. In the high-rise & low-rise mixed building groups, the wind at high altitude was intercepted by high-rise buildings and returned to the ground according to the down washing phenomenon, leading to strong winds between high-rise buildings [2].

In terms of building form, Hang et al. analyzed two kinds of urban models composed of 4 (2*2) or 16 (4*4) buildings. They explained that adopting semi-open building roofs can significantly promote the natural ventilation of the buildings [18]. Tsang found that building podiums affect the natural ventilation at pedestrian height [16]. Adamek et al. successfully improved the downwash effect of high-rise buildings by utilizing the influence of podiums [2].

Concerning the windward side, Tsichritzis et al. compared more than 20 building plans on the same site. They found that increasing the frontal area ratio (defined by the area of the building's vertical surfaces facing the approaching wind divided by the entire plan area) will dramatically affect the wind speed of the outdoor space [19]. Based on the concept of Frontal Area Density, Tong Ma et al. studied 36 residential areas in Tianjin and concluded that wind speed and calm wind area ratio are negatively correlated with frontal area density and site coverage [20].

These studies present requirements for the parameter configuration of buildings from different perspectives. The wind environment of buildings will be affected jointly by multiple factors, such as building coating coverage rate, building spacing, building height, building shape, and building windward surface. However, the comprehensive and interactive influence of these factors on building layout is still under-studied.

The second category emphasizes the wind conditions of building layout schemes, especially on the optimal layout mode development based on the local climate conditions by comparing different layout schemes on the same site. Asfour et al. studied the wind conditions of several residential building layouts in different wind directions. A well-designed configuration provides better ventilation conditions, i.e., buildings are set around the central space with an opening side of the layout to the prevailing wind direction [21]. According to this, Hong et al. applied the outdoor thermal environment simulation platform (SPOTE) to test the effects of different building layout patterns and tree arrangement patterns on outdoor wind environments and thermal comfort at outdoor pedestrian height in residential areas. The horizontal vortex at the edge of buildings will be accelerated when the long building facade is parallel to the prevailing wind direction, so a pleasant wind environment will be consequently obtained at the pedestrian height [6]. However, taking southern China as an example, if the long facade of the building is parallel to the prevailing wind direction in summer (southeast), sunshine conditions are unqualified for residential needs. Thus, this experience is not universally applicable for all residential areas.

Compared to western urban morphologies, contemporary Chinese residential layouts often possess several differences including larger plots, more regular layout patterns, higher building density, and higher buildings. This makes it worthwhile to study Chinese residential areas, especially for southern China. Hu et al. studied a typical residential area scheme in Shanghai. They proposed the concept of passage ratio as a design parameter for urban ventilation to evaluate the influence of a building layout on the average ventilation efficiency [22]. Based on this, Li et al. innovatively developed a wind network index to evaluate the impact of building layouts on the wind environment and verified its effectiveness through wind tunnel experiments [23]. Ying et al. explored the influence of building orientation on the wind environment in 6 residential case studies in Hangzhou [3].

For northern China, the residential areas' wind environments are also studied. Shui et al. studied 7 residential areas in Harbin, a colder region of China, and proposed that the building height should be strictly controlled, and that mixed & closed layouts are highly recommended [24]. Ma et al. studied the wind environment of 36 residential areas in Tianjin. They proposed that an optimized building layout for Tianjin city comes from the combination of mixed mid-to-high-rise parallel layout and mid-to-high-rise buildings according to its climate [20].

The current research on residential areas in southern China is focusing on the orientation and architectural layout types. Currently there is a gap to explore the automation of optimized layout generation for southern China. In contrast, the wind environment in northern China is more comprehensively studied with computational methods proposed for an automatic building layout generation. This study seeks to address this gap via the comparative study of architectural layout schemes with a focus on wind environments of high-rise building layout schemes in high-density residential areas in China.

2.2. Intelligent layout optimization with Genetic Algorithms

With the development of generative design, various heuristic algorithms have been applied to solve the complexity and optimization issues of layout designs. Genetic Algorithms (GA) are one of the most classic heuristic algorithms adopted in architecture.

For energy consumption problems of medium-sized hospitals, Ancona et al. used the GA Trigen 3.0 to study the optimal compliance allocation of energy systems based on objective minimization. The EGO (Energy Grids Optimization) program, based on GA, achieved optimal solutions of energy and economy by using multi-objective optimization problems [25]. Talha et al. used GA to optimize the frame structure of high-rise buildings. With the help of CSi open application programming interface (SAP2000 OAPI) code and GA, the structural design method of high-rise buildings based on strength and stiffness was coded in MATLAB. The feasibility of optimal solutions was compared via complexity index parameters [26]. For the optimization of wind environment conditions, Mosetti et al. used GA to analyze the layout optimization of wind power stations. A detailed wind turbine layout plan was developed by maximizing wind power generation through optimizing the location of each wind turbine [27]. For a similar research focus, Grady et al. acquired better results by raising the number of individuals and iterations of three wind simulation models [28]. Ju et al. proposed an improved GA that combines machine learning and CFD to optimize a wind power station layout [29]. Since then, a series of meta-heuristic and mathematical programming algorithms have been proposed and fully studied, such as the particle filter method [30], simulated annealing [31], random search [32], mixed integer programming [33], convex programming [34], global optimization strategy [35], or the Coral Reef algorithms [36]. However, GA are still one of the most popular methods due to their advantages of a high efficiency and easy implementation. In our study, this algorithm is applied to automatically generate building layouts.

In building layout optimization, various improved algorithms and platforms have been proposed by scholars to provide design guidance for generating the best layout scheme. Ren et al. studied the maximum plot ratio problem in the planning stage of a residential area from the perspective of sunshine analysis. By using the improved GA, they calculated the maximum envelope solid of the building block [37]. Wei et al. developed a cyber-physical experimental platform for general real-time dynamic model updating, significantly promoting the research of building optimization [38]. Nguyen et al. analyzed the simulation-based optimization methods used in the architecture design field. They provided a research vision in the demand for efficient approximation methods and alternative models to reduce uncertainty in optimal solutions [39]. Inspired by this, Araghi et al. created a computational design strategy via the generative calculation method of Cellular Automata (CA). Although this strategy benefited the early stages of the design process by addressing accessibility and lighting requirements, it overlooked the influence of the wind environment on building thermal physical properties [40]. Zhang et al. studied the impact of urban morphology on air temperature. They aimed to improve the urban thermal environment in the cold regions of China through a novel urban morphology optimization strategy cooperated with the SPEA-2 algorithm. Nevertheless, this strategy shows regional limitations for later-on general application cases [41].

In studying automatic optimization of high-rise residential layouts based on wind environments, Du used the multivariable optimization method to study the layout optimization of lift-up buildings. He proposed a multivariable optimization method that coupled CFD simulation and a RSM technique to optimize the wind comfortability by modifying the geometric configurations of lift-up design [42]. Xu et al. applied GA to study the urban layout optimization method in the cold region city of Shenyang. They proposed a parameterized platform based on Grasshopper and adjusted the urban form for the improvement of the urban microclimate [43].

Zhang et al. developed a multivariate linear regression model to study the correlation between temperature and urban form in the cold region city of Harbin. They proposed a multi-objective optimization framework to address the regional microclimate [41]. In recent years, an increasing number of works have adopted computer algorithms to explore automatic generation methods of building layouts. However, these studies were only carried out in cold region cities and focused on large-scale urban buildings under those climatic conditions. Additionally, the building scale is too rough to simulate and optimize small-scale residential buildings.

Hence there is space for improvement to study the automatic optimization of high-rise residential layouts with a high precision. Here, deep learning technologies are adopted to assist the layout planning of residential areas. It exhibits promising potentials in the residential area design in the layout planning stage to improve the outdoor wind environment of buildings.

2.3. Wind environment prediction with neural networks

Deep learning is a data-driven approach that iterates and optimizes an error function with the aim to solve a target problem. Le Cun proposed Convolutional Neural Networks (CNN) [44], which is currently the most widely used in various deep neural networks. CNN was first used in face detection [45,46], face recognition [47] and character recognition [48] problem solving for visual processing. In general, the front end of the multi-layer convolution layer is set to a shallow convolution layer with a smaller perceptual domain to learn the details of the image (such as the shape and color features of the learning object) [49]. The back end is set to a deeper convolution layer with a larger perception domain, which is used to learn the abstract features of the research object (such as the direction, location, and size information of the object). At present, CNN has been widely used in image detection and image classification. Long J et al. proposed a Fully Convolutional Neural Network (FCN) [50]. FCN uses a convolution layer instead of a full connection layer as in CNN, which is a further optimization of standard convolution networks. Since FCN uses a deconvolution layer for up-sampling operation, the output size of the model can be the same as that of the original image, so it does not require restrictions on the size of the input image.

Aiming at the prediction of climate and environment, Junmo Koo et al. divided reference sites and target sites into three geographical categories: Korean plain, coast and mountains. Using the wind speed data of the reference station of an Artificial Neural Network (ANN), the accuracy of wind speed prediction at the designated target site was studied. By calculating the error of the wind speed data obtained from the ANN and CFD simulations, the reliability of the ANN model in wind speed evaluation was verified [51]. Mousa Afrasiabi et al. designed an approach based on deep learning to predict the probability density function of wind in the next few hours. At the same time, CNN was used to enhance the learning of spatial characteristics, and a gradient-based loss function was proposed. The effectiveness and superiority of the proposed probabilistic wind speed prediction were verified by two actual data sets of London and Iran [52]. Jinle Kang et al. predicted precipitation in Jingdezhen using a Long Short-Term Memory (LSTM) network model based on meteorological data from 2008 to 2018, and compared its performance with other classical statistical algorithms and machine learning algorithms. The experimental results show that LSTM is suitable for meteorological prediction and can provide sufficient time for formulating strategies to deal with potential related disasters [53]. Manoj Verma et al. used five parameters, namely relative humidity, wind direction, ambient temperature, environmental pressure and perceived water, and used ANN and the Multiple Linear Regression technology (MLR) to predict wind speed in the study area [54]. Wang et al. designed a hybrid model of Wavelet Neural Network optimized by Genetic Algorithm (GA-WNN) based on Variational Mode Decomposition (VMD). A prediction system composed of data preprocessing, integration strategy and multiple single models was designed to predict wind speed in wind power generation to reduce the influence of wind speed characteristics on power grid operation decisions [55].

In this study, deep learning technologies are used to predict the wind environment of the building layout with the same size as the input building layout map. It shows a good application prospect in the design of residential area layout at planning stage and an improvement of the outdoor wind environment of buildings.

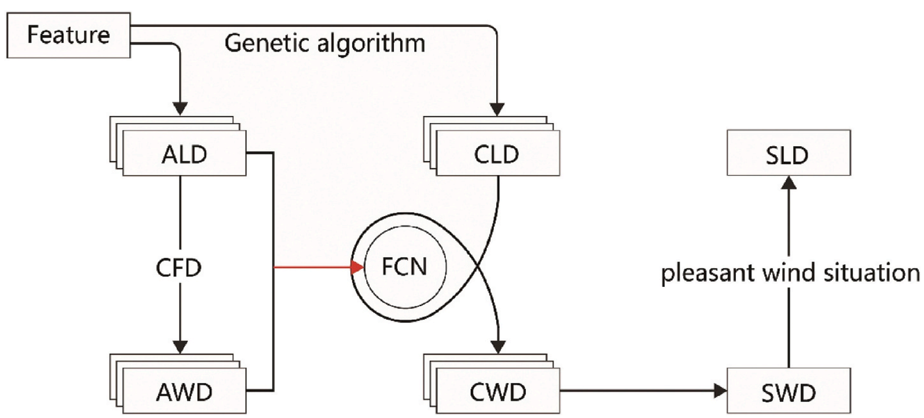

Fig. 1. Framework of intelligent planning method to optimize the high-density residential layout with given wind environment.

3. The framework and the Operation Process of the intelligent planning method

3.1. General framework of the intelligent planning method

There are seven-part databases forming the framework of the intelligent planning method for optimizing the wind environment of the residential layout (Fig. 1).

Part 1 Feature Database: Feature Extraction of High-Density Residential Areas. The samples of high-density residential areas in the study area are collected. The plot data of specific buildings are extracted from plot size, floor area ratio, building size, and building height. Then the layout mode is recognized according to building group division in these specific samples.

Part 2 Artificial Building Layouts Database (ALD): Generation of the Artificial Layout Model. According to the requirements of building specifications, sunshine spacing and fire spacing, the ALD in the frame diagram is developed based on the summarized data and layout scheme.

Part 3 Artificial Building Layouts' Wind Environment Database (AWD): Wind Environment Simulation by CFD. The annual wind speed, direction, and frequency data of the study area are collected. Differences between the wind in winter and summer with the disparate external physical environment of the buildings is anticipated. In this study, the wind direction and speed data of the maximum wind frequency in winter and summer are summarized separately. Additionally, the wind environment of the highest profit scheme based on government limitations is also modeled and simulated via the CFD software PHOENICS.

Part 4 Computational Building Layout Database (CLD): Generation of the Computational Layout Model. With the building data, plot data, and building layout summarized in Part 1, the computer expansion scheme is generated by the GA. The equation of the GA is controlled according to the minimum spacing between buildings complying with residential criterions. The formula that generates a building layout with high fitness is selected.

Part 5 Computational Building Layouts' Wind Environment Database (CWD): Generation of the Wind Environment by FCN. The ALD and the corresponding AWD are processed into matrices related to quantity and position. Then the coupling relationship between ALD and AWD is studied by FCN. The wind environment of CLD is predicted through established FCN model.

Part 6 Satisfied Wind Environment Database (SWD) and Part 7 Satisfied Building Layout Database (SLD): Selection of Satisfactory Computational Layouts. The satisfied residential building layout schemes are filtered by evaluating the satisfied corresponding wind environment.

These seven parts of the database are organized along the lines of training set preparation, validation set testing, and optimal set selection, which constitute the framework of the intelligent planning method.

3.2. Key operations of the intelligent planning method

3.2.1. Layout generation

The building layout schemes are normally expressed in Computer Aided Design (CAD) form as the layout planning of buildings is two-dimensional. Therefore, the layout scheme is divided into uniform 5 m*5 m grids, in which the value of the grid represents the height of buildings. In this way, a large matrix is established to express the layout of buildings in planar form.

In the automatic generation stage, the single building is automatically and randomly placed in the plot area as the parameters of building layout are input, including building size, height, quantity, and a specific building group division scheme of the layout. This step ensures that all buildings fit into the layout without overlap.

The GA is applied in the automatic generation of the building layouts to achieve an optimized distance between buildings. Without satisfactory distance between buildings, a waste of land resources (larger space), and the unexpected wind environment and sunshine in building groups can occur. This study is based on the penalty and fitness functions of the designed GA, as shown in formulas (1formulas (1) and (2)(2).

$$P_i = \frac{M_i^d}{T_i^d + 1} \tag{1}$$

$$F = \left[\sum p_i + 1\right]^{-1} \tag{2}$$

where P_i represents the penalty value of the building i; T represents the actual distance between buildings, d represents the directions, i.e., east, west, south, and north, T_i^d represents the actual distance in the d direction; M represents the minimum distance between buildings, M_i^d represents the minimum distance in the d direction; F represents the fitness value of the whole layout; ΣP_i represents the sum of the penalty values of all buildings in the layout.

For a single layout, the penalty values for each building and the total penalty value for all buildings are calculated. The penalty value of a single building is the ratio of the minimum building distance in four directions to the actual building distance. The fitness of the building is defined as the reciprocal of the penalty value. And the fitness of the whole layout is the sum of the fitness of N buildings.

These two formulas show how the actual spacing between buildings, the minimal spacing and the degree of adaptation are related. The closer the actual spacing is to the minimal spacing, the more adaptable it will be. In contrast, too much or too little spacing reduces the layout's flexibility, making it more likely to be eliminated. The abandoned layouts will not participate in the next round of optimization, which ensures that the algorithm is updated towards an optimal solution. After several rounds, the fitness converges to a stable value with a corresponding optimal layout. The threshold value for fitness is set to 100, and the optimization process is terminated if the worst fitness of a newly generated layout reaches 100. Then, the optimized layout library is obtained by ranking fitness in a decreasing sequence.

In addition, the number of iterations is set to 300, the starting population size is set to 50/100/200, the variation rate is set to 0.3, and the top 20 mutant outcomes are chosen for a two-by-two crossover.

3.2.2. Generation of wind environment corresponding to layout

Due to the various building layout schemes in the same plot, the corresponding wind conditions will be complex and diverse. The neural network model can automatically update the weight by inputting different parameters, based on the coupling relationship between building layout and wind environment. In the initial stage, the neural network can find this relationship by learning from a limited number of samples. In the later stages, the wind environment predictions can be quickly generated based on learning experience for various layout schemes.

To solve the time-consuming problem of traditional software simulation, a FCN is proposed as an alternative model for wind speed prediction. It emphasizes the quick prediction of wind speed for the optimized building layout within a permissible error.

In machine learning, models improve their robustness by learning the characteristics of data. Usually, feature engineering, an essential component before model training, determines the quality of model training results. However, in this study, the feature engineering for a spatial layout is challenging to come by, which restricts the extraction of the layout characters of buildings and the relationship characters between adjacent buildings. Hence, the establishment of a regression prediction model by using the traditional machine learning methods becomes a problem. Therefore, the input of this study has been converted from a three-dimensional layout to a two-dimensional layout plane image, with the modeling completed by the FCN.

Fig. 2 shows the network structure used. The model includes nine convolution layers that can be roughly divided into the encoding layers and the decoding layers. In the encoding layers, the structural characters of the layout plane are extracted through four convolution layers with an input of images. Then, a feature vector containing the building layout information is collected. More and more information on building layouts is achieved by this pixel-vector conversion process. In the decoding layers, the feature vectors obtained from the encoding part are converted and restored to the input size by the remaining three convolution layers. In the end, the predicted wind speed of each pixel can be obtained.

3.2.3. Assessment of wind comfort

Chinese architecture norms have standardized the wind environment condition around buildings. The Design Standard for Green Building [56]. Stipulates that the wind speed of the pedestrian area outside a building should not exceed 5 m/s under winter wind conditions, and the wind speed ratio outside the building (the wind speed at the measuring point divided by the initial wind speed) is less than 2. Under the wind conditions of spring and autumn in the transition seasons and hot summer, there should not be a windless area or wind vortex in the pedestrian area around the building.

In this study, the predicted wind speed is to conform to those comfort levels. The wind speed ratio is used to evaluate the comfort of the wind environment. If the wind speed ratio is greater than 2.0, there will be safety hazards, and it does not meet the requirements of the Green Building Standards. If the value is less than 0.5, there will be a still wind area, which is not conducive to airflow flow. Therefore, the screening process based on comfort levels follows two steps: Firstly, layouts with wind speed ratios greater than 2.0 are eliminated; secondly, the areas with wind speed ratios of less than 0.5 are counted, as these points inevitably appear in each layout scheme. The overall statistical data are displayed in the software interface to facilitate the decision making of architects.

3.2.4. Test of wind prediction

The key to machine learning is to narrow the gap between the predicted value and the real value as much as possible, and to finally obtain an optimal solution from the algorithm. The Mean Square Error function (MSE) is the most widely used in early image reconstruction tasks, and it is also a loss function as the default choice. It is widely used in machine learning and can be used for reinforcement learning and other specific problems. The loss function can evaluate the modeling accuracy of the algorithm by minimizing the objective function. After the FCN model is built, a loss function is needed to evaluate the prediction effect of the model. In this research, MSE was used as a loss function to evaluate the error between the wind speed simulated by PHOENICS and the FCN

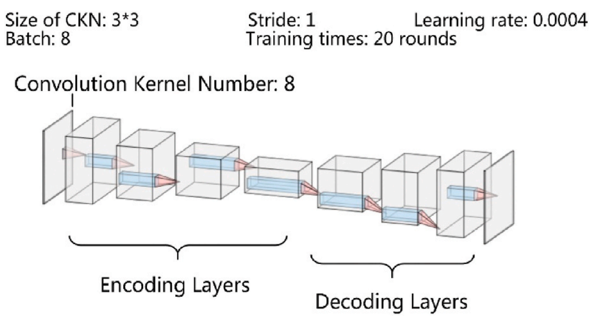

Fig. 2. Network structure of CFD agent model based on FCN.

predicted wind speed, calculated by Formula (3).

$$MSE = \frac{1}{n}\sum_{i=1}^{n}(y_{PHO} - y_{FCN})^2 \tag{3}$$

In formula (3), n represents the number of cells in a layout; y_{PHO} represents the simulated wind speed value of PHOENICS, y_{FCN} represents the predicted wind speed value of FCN. The smaller the MSE value, the higher the accuracy of the prediction model.

4. Case study

4.1. Data preparation

Although the computer dominates the specific operational process of all typical layout production and satisfied layout selection, the input data must rely on the architect's predetermination based on the regional characteristics. It includes the building model data and the regional wind environment parameters. These two forms of data must be presented together.

4.1.1. Building model

Most architectural forms found in high-rise residential areas can be divided into board-type buildings and point-type buildings (or tower-type buildings), and those two base plan forms have different spatial characteristics and applicable situations. The plans of board-type buildings in Southern China are commonly oriented along the east-west direction. The house type is characterized by a large south-facing width and short depth. This can make each unit connected from north to south for cross ventilation, which is conducive to indoor air circulation. The point-type has little difference between width and depth, and the house type design has higher requirements for an architect's experience and a higher difficulty for design. The plan geometries of point-type housing are mainly T-shaped, rectangular, cross-shaped and butterfly-shaped. In terms of layout, site corners can be used whenever possible.

This study selects three economically developed cities in the Yangtze River Delta - Shanghai, Nanjing and Hangzhou, as sample cities, with 25 typical mixed residential areas as reference studies. The overall planning and corresponding building data of the references are shown in Fig. 3 and Table 1. In this study, the plot size, plot proportion, building size, height and layout of the residential area in the references are analyzed.

Based on Code for Fire Protection Design of Buildings [57], the height of the case study buildings is set to 11 stories (33 m), 18 stories (54 m) or 30 stories (90 m). Through the investigation of the number and size of individual buildings in the 25 reference studies, Table 2 is generated. There are five types of slab buildings, represented by B, and three types of point buildings, represented by P.

Since the land area and plot shape of the references are different, the number of individual buildings in the layouts also differs. In the selected references, the largest land area, number xx, is 100,000 square meters, with a floor area ratio of about 2.5. The long blocks in the south accounts for the majority. The research case study is a mixed residential area. Through the investigation and summary of the individual buildings and layouts of the reference studies, the case study land area is set to 390 m * 240 m, and the volume ratio is placed within 2.6–2.65. To avoid the disorderly arrangement of buildings with different heights and sizes, the land is divided into four

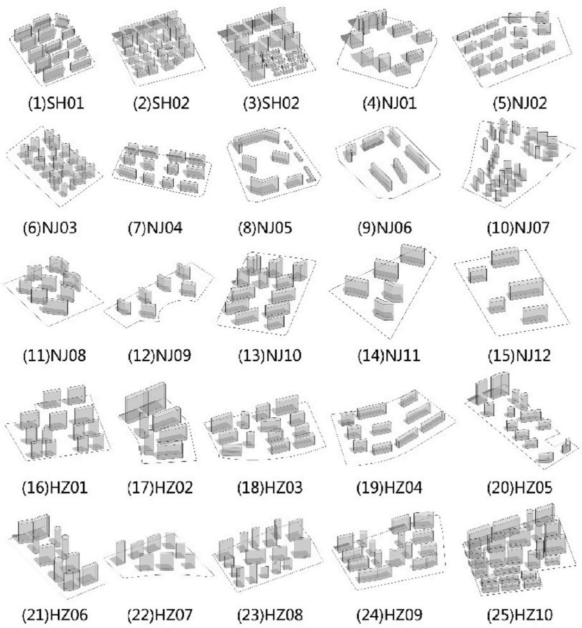

Fig. 3. Diagrams of the reference studies.

Table 1
Building data of the reference studies.

Number	Name	Built year	Land area (hectare)	Building area (hectare)	Plot area
1	SH01	2015	4.1	8.2	2.00
2	SH02	2015	12.9	29.5	2.29
3	SH03	2017	8.1	19.4	2.40
4	NJ01	2013	3.9	8.2	2.10
5	NJ02	2017	8.0	16.0	2.00
6	NJ03	2013	9.6	21.1	2.20
7	NJ04	2014	7.3	19.7	2.70
8	NJ05	2014	4.2	10.6	2.52
9	NJ06	2010	4.3	10.0	2.36
10	NJ07	2014	8.7	20.1	2.30
11	NJ08	2014	3.6	8.0	2.20
12	NJ09	2008	3.1	9.0	2.92
13	NJ10	2008	6.6	14.9	2.27
14	NJ11	2010	3.2	7.14	2.23
15	NJ12	2015	1.8	3.6	2.00
16	HZ01	2006	4.8	13.0	2.70
17	HZ02	2007	4.6	16.1	3.50
18	HZ03	2006	6.9	15.9	2.30
19	HZ04	2006	4.2	9.7	2.30
20	HZ05	2008	6.3	15.8	2.50
21	HZ06	2004	5.9	21.2	3.60
22	HZ07	2014	10.7	32.1	3.00
23	HZ08	2008	9.6	24.0	2.50
24	HZ09	2008	7.1	19.9	2.80
25	HZ10	2007	6.6	17.4	2.64

Table 2
Adopted building types.

Building type	Number	Plane size/m	Layer number/F
Slab-type apartment	B1	60*15	11
	B2	40*15	18
	B3	60*15	
	B4	40*15	30
	B5	60*15	
Point-type apartment	P1	20*15	11
	P2	20*15	18
	P3	20*15	30

groups: 'green space and roads', 'P1/P2/P3 buildings with plan size of 20 m * 15 m′, 'B2/B4 buildings with plan size of 40 m * 15 m′, and 'B1/B3/B5 buildings with plan size of 60 m * 15 m'. The research focus is on the layout of residential buildings, hence in this stage, the inclusion of public buildings such as schools is not considered. Examples of land division schemes for the point-plate hybrid are shown in Fig. 4. It follows the principle that the point building is set on the south side, and the plate building on the north. The building height from south to north is arranged from low to high.

The distance between buildings is carefully controlled to meet the building lighting standards and fire protection requirements of Code for Fire Protection Design of Buildings [57] and the sunshine simulation results of the Tianzheng CAD software. Table 3 shows the specific constraint values.

The scheme design was carried out according to the above research. In each scheme, two kinds of point block building and two types of slab block building in the south direction were included. Finally, 179 plot ratio combination schemes and 880 plane layout schemes have been obtained as artificial models.

4.1.2. Wind simulation

The appropriate wind environment does not only promote ventilation and heat dissipation in summer, but also reduces cold wind in winter. Compared to the transitional seasons, the environment in winter and summer will have a larger influence.

At the same time, the requirements of wind speed and wind pressure in summer and winter are stipulated in the Design Standard for Green Building [56]. Therefore, this study selected winter and summer as the target seasons. The wind speed, wind direction and wind speed frequency data of the reference cities are analyzed and summarized in Table 4.

According to the data of the three reference cities, the wind speed is set as 3 m/s with the south (summer monsoon) and north directions (winter monsoon).

The wind simulations are carried out by PHOENICS on the obtained building model database, ignoring surrounding buildings. The 3D calculation domain is set to 3 times the 3D dimensions of the plot (i.e. X * Y *Z = 1170 m * 720 m * 270 m). The grid for the

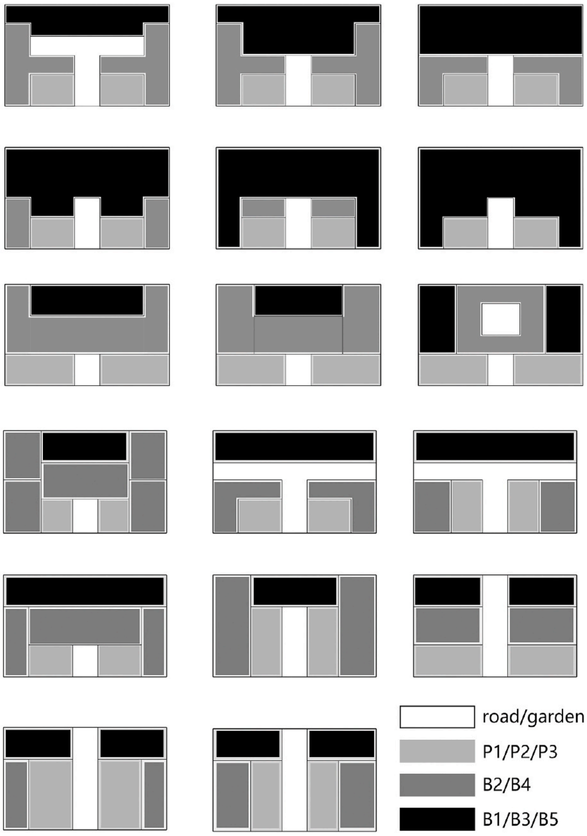

Fig. 4. Group division plan of point-slab mixed high-rise residential area.

Table 3
Distance between buildings for different building types.

Plane size/m	Number	Layer number/F	North-South distance/m	East-West distance/m
40*15	B2	18	33	13
	B4	30	40	13
60*15	B1	11	44	13
	B3	18	48	13
	B5	30	63	13
20*15	P1	11	16.3	13
	P2	18	17	13
	P3	30	17	13

Table 4
Seasonal maximum frequency wind environment data of the three sample cities [58].

City	Season	Maximum frequency wind direction	Frequency of wind direction/%	Average wind speed of maximum frequency wind direction m/s
Shanghai	spring	ESE (112.5°)	11.91	3.8
	summer	ESE (112.5°)	14.96	3.4
	autumn	NNE (22.5°)	14.41	3.8
	winter	NNE (22.5°)	14.24	3.5
Nanjing	spring	ESE (112.5°)	9	3.8
	summer	SE (135°)	8	3.4
	autumn	E (90°)	12	3.6
	winter	NE (45°)	10	3.5
Hangzhou	spring	ESE (112.5°)	8.86	2.2
	summer	SWS (202.5°)	9.55	2.3
	autumn	E (90°)	7.73	2.0
	winter	NWN (22.5°)	10.94	2.2

simulation is set at a density of 5 m * 5 m, with X * Y *Z grid number 78 * 48 * 41. The Standard k-ε (Standard k-epsilon) equation is used for calculations considering both south (summer wind direction) and north (winter wind direction) wind. The climate type is subtropical monsoon, and the air is set to 1.013 kPa and 20 °C. No model surface roughness is set because the scale of the model is residential. The number of calculations is set to 2000 in order to obtain a better convergence of the results. At the conclusion of the simulation, the wind data at a pedestrian height of 1.5 m are exported for each scenario.

Based on the wind data simulated above, this study selects eleven wind speed measurement points to analyze the typical wind environment of ALD. All the measurement points are distributed in places with frequent residents' activities, such as entrances and exits of the compound or the centres of the building groups and the green belts, as marked by red dots in Fig. 5. Both ALD and AWD training databases are obtained during these processes.

4.1.3. Visual data integration

A CAD plan of layout is converted into a matrix representation of 5 m * 5 m cells that stores information about the building's position and height. It turns the graphical data into a digital representation, which makes further analysis more convenient.

Each layout plan can have up to 60,000 wind speed data points, although the difference is subtle. It is necessary to clean the wind speed data. Based on the idea that the wind speed data must correlate to the building layout data, the wind speeds are separate into a matrix of 5 m * 5 m cells, and utilized the average wind speed value for each cell.

Then the ALD is obtained as well as AWD, and each database is separated into a training set and a test set in a 7:3 ratio. As an example, the building layout illustrated in Fig. 6 can be represented by the matrix as Fig. 7 and the wind environment data of this scheme as Fig. 8.

4.2. Sample results and validity verification

4.2.1. The building layout optimization comparation

To verify the effect of the GA, 8 B1 buildings, 9 B2 buildings, 6 P1 buildings and 6 P3 buildings are chosen as sample. Figs. 9 and 10 show the layout before and after optimization respectively.

A comparison with these two figures shows that the relative positions of specific buildings have changed significantly after optimization during the crossover process of the GA. At the same time, the positions of some buildings have changed slightly during the mutation process. Overall, the optimized building plan is more in accordance with the practical requirements, and the land use efficiency is improved while meeting the daylight distances.

The wind environment is simulated based on the optimized sample layouts, and areas are counted with suitable wind conditions in summer and winter according to the wind speed ratio of 0.5–2. The percentage of acceptable measurement points for this layout is 82.35% in summer and 80.70% in winter. Referring to Soligo's comfort assessment [59], a layout is considered comfortable if the probability of a comfortable wind speed is above 80%. This optimized layout therefore shows a good comfort level in both summer and winter. Figs. 11 and 12 illustrate the wind environment simulations for the optimized layout in summer and winter respectively. Table 5 shows the wind statistics for the optimized layout.

Fig. 13 shows the software interface for this case study. 10 building layout schemes are automatically generated for architects to develop as layout prototypes. This can effectively solve the problem of being heavily influenced by the architect's experience, resulting in less comprehensive solutions.

4.2.2. Wind speed prediction verification

By using the MSE, formula (3), to calculate the network prediction value and real value of the model, the loss function diagram of the algorithm model built in this study is obtained. The change trend of MSE during the training is shown in Fig. 14. In general, this error shows a downward trend after training. In the first six rounds, the error reduction gradient is greater than the following parts.

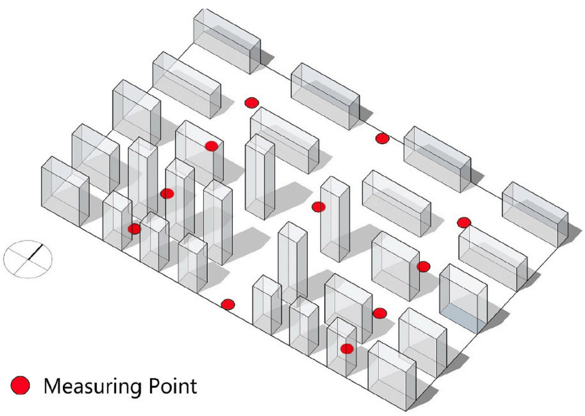

Fig. 5. Location of measuring points.

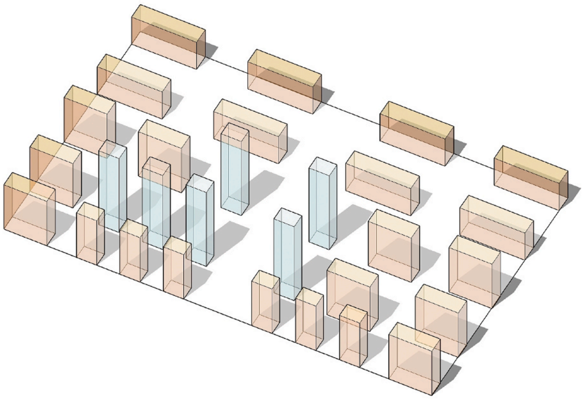

Fig. 6. Layout of building scheme represented in 3D.

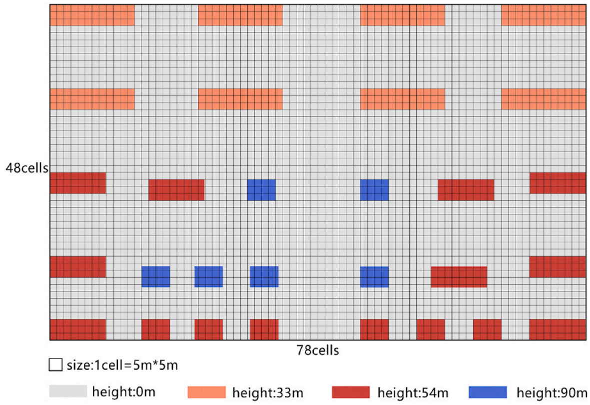

Fig. 7. Layout of building scheme represented by matrix.

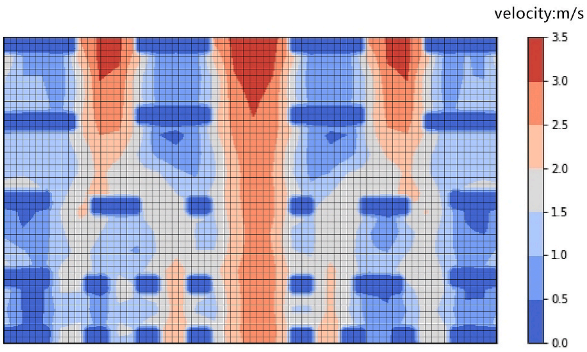

Fig. 8. Wind environment data of the scheme.

After 12 rounds of training, this error changed little. The training effect therefore reached the expected optimal solution. After 15 rounds of training, the mean square error (MSE) of the model on the training set is about 0.13, and the error on the test set is about 0.16.

The wind speed data used in the experiment is 3 m/s. Under the test error of 0.16, the error value of the wind speed is about 0–0.48 m/s. According to the requirements of 3.2 in Inspection and Quarantine of China, Specifications for Surface Meteorological Observation [57], the allowable error range of wind speed observation data from meteorological stations is 0.5 ± 0.03 m/s. The wind speed error in this study meets the requirements of the standard. The effect of the model prediction under different parameters is further compared through experiments, as shown in Table 6. The results show that the minimum batch size is helpful to the best effect of the model. At this time, the MSE distribution of the test sample is about 0.16.

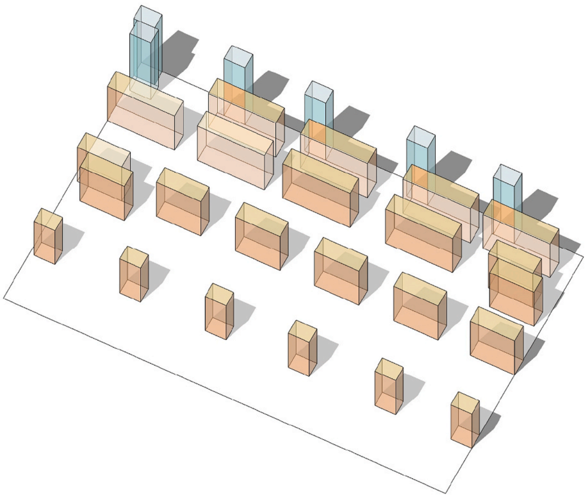

Fig. 9. Layout of sample model before optimization.

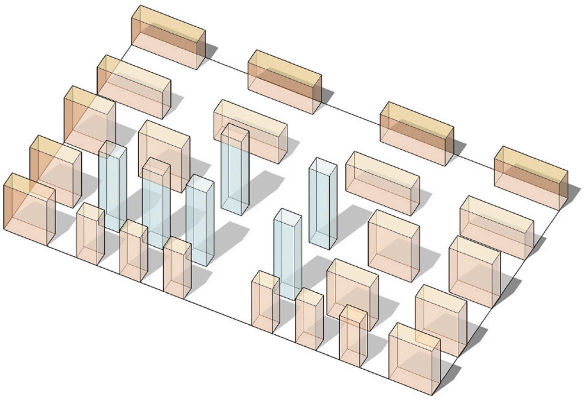

Fig. 10. Layout of sample model after optimization.

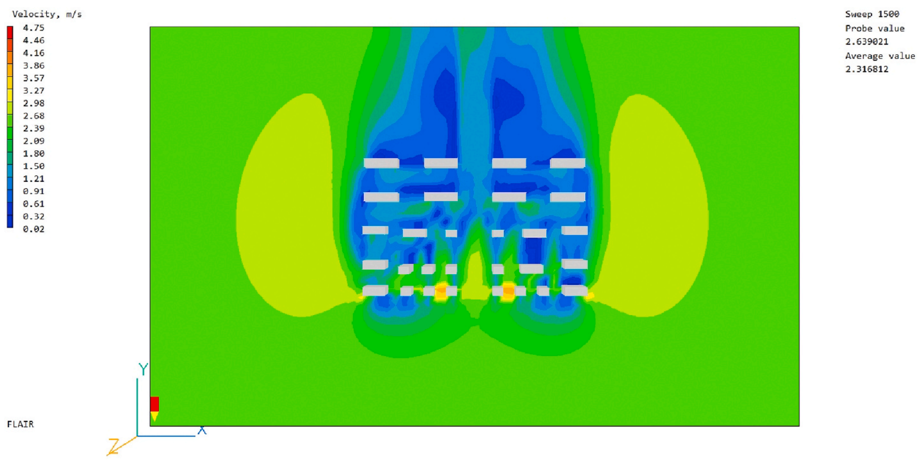

Fig. 11. Summer wind environment data of optimized residential layout.

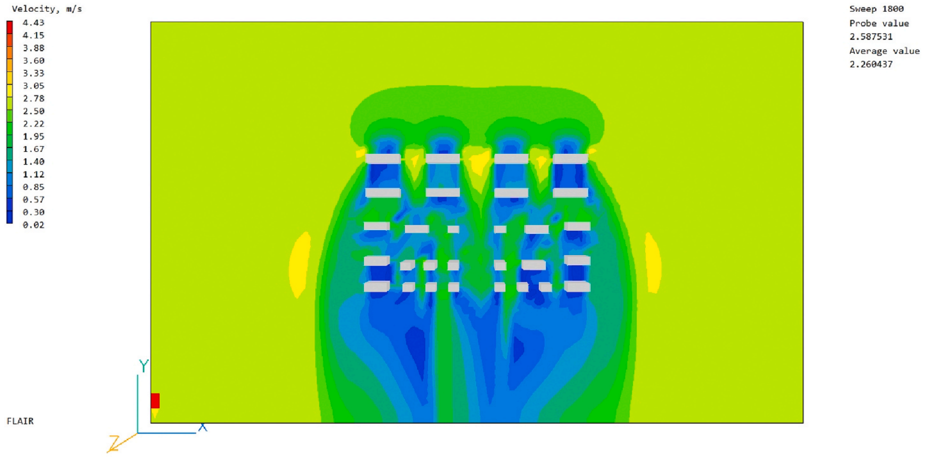

Fig. 12. Winter wind environment data of optimized residential layout.

Table 5
Wind environment statistics of the optimized layout (1.5 m above ground).

season	Number of comfortable measuring points ($0.5 \leq$ wind speed ≤ 2)	Total number of measuring points	Proportion of comfortable measuring points
summer	55511	67405	82.35%
Winter	55008	68161	80.70%

The comparison between the time efficiency of the PHOENICS simulation and FCN prediction is presented in Table 7. Although it takes 1 h to process the training of the model, only a few seconds are needed to predict the wind environment of a layout thereafter. Compared with the simulation using PHOENICS, the proposed FCN model features excellent time-efficiency improvement that has achieved the expected results.

5. Conclusions

In this study, an intelligent planning method is proposed to automatically generate and filter the high-rise buildings layout plans for residential areas with comfortable wind environment. It integrates two deep learning algorithms, GA and FCN. All types of layout plans are automatically generated by GA. The wind environments of previous layout plans are quickly predicted by FCN. Finally, the high-rise buildings layout plans for residential areas with comfortable wind environment are identified for further developing by architects. This method seems to be capable of meeting the application requirements in terms of accuracy and speed through the validation of the cases in Shanghai, Nanjing and Hangzhou in China.

There are two significances. Firstly, it replaces the traditional individual wisdom with group wisdom through deep learning algorithms on the primary stage of high-rise building layout planning for residential area, enhances the comprehensiveness and optimization of the solutions, and breaks the limitation caused by the architect's personal experience-driven planning. Secondly, compared with traditional wind environment simulation approaches, it overcomes computational power and efficiency constraints, allowing for wind prediction of large-scale multiple scenarios to be completed in a matter of seconds with acceptable forecast error.

This study also has some limitations. The data used for the case validation, such as plot size, plot volume ratio, and wind speed, are only predetermined based on actual case studies in the Yangtze River Delta region in China. The generalizability and precision of the method can still be improved because the cases are concentrated in a single area and are relatively few in sample size. The further study will build a database including parcel size, parcel shape, volume ratio, wind speed, wind direction, etc. The database will be continuously supplemented from both cross-regional and multi-sample to optimize this method.

Author contribution statement

Xiaoyu Ying: Conceived and designed the experiments; Performed the experiments; Contributed reagents, materials, analysis tools or data.

Xiaoying Qin: Conceived and designed the experiments; Performed the experiments; Analyzed and interpreted the data; Contributed reagents, materials, analysis tools or data; Wrote the paper.

Liying Shen: Analyzed and interpreted the data.

Chunyang Yu: Conceived and designed the experiments; Wrote the paper.

Jia Zhang: Conceived and designed the experiments; Contributed reagents, materials, analysis tools or data; Wrote the paper.

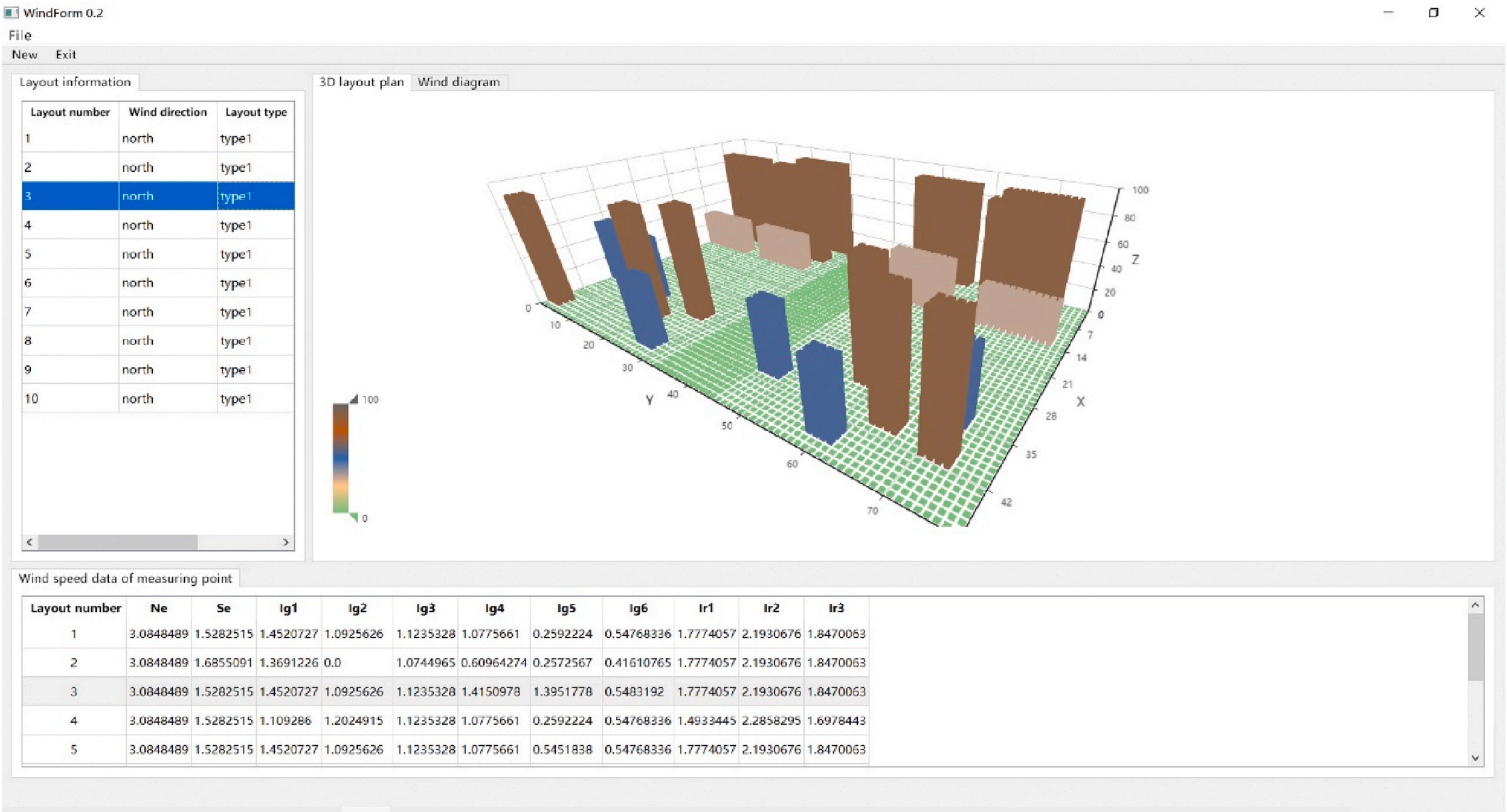

Fig. 13. Interface of software calculation result under-sample parameters.

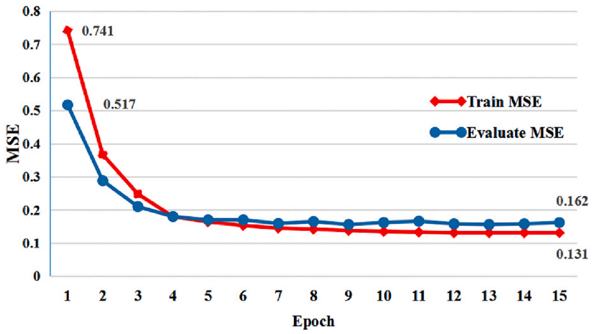

Fig. 14. Change trend of MSE during model training.

Table 6
Performance of GA with different parameters.

Epochs	Batch Size	Learning Rate	CPU Time (min)	Training MSE	Validation MSE
15	32	0.0004	57.85	0.336	0.362
15	16	0.0004	63.42	0.152	0.175
15	8	0.0004	65.96	0.142	0.166
15	32	0.001	50.50	0.145	0.169
15	16	0.001	50.85	0.140	0.167
15	8	0.001	52.85	0.131	0.162

Table 7
Comparison of time efficiency between software simulation and model prediction.

Method	Training time/h	Layout evaluation time/s
PHOENICS	–	600–1200
FCN model	≈1.0	≈1.07

Funding statement

Dr. Xiaoyu Ying was supported by National Natural Science Foundation of China [51878608], Natural Science Foundation of Zhejiang Province [LY18E080025].

Dr. Jia Zhang was supported by Centre for Balance Architecture of Zhejiang University [KH20212791].

Data availability statement

Data included in article/supp. material/referenced in article.

Declaration of interest's statement

The authors declare no competing interests.

References

[1] T.V. Lawson, The effects of wind on people in the vicinity of buildings [M], in: Proceedings 4th International Conference on Wind Effects on Buildings and Structures, Cambridge University Press, 1975, pp. 605–622.
[2] K. Adamek, N. Vasan, A. Elshaer, et al., Pedestrian level wind assessment through city development: a study of the financial district in Toronto [J], Sustain. Cities Soc. 35 (2017) 178–190.
[3] X.-Y. Ying, G. Ding, X.-J. Hu, et al., Developing planning indicators for outdoor wind environments of high-rise residential buildings [J], J. Zhejiang Univ. - Sci. 17 (5) (2016) 378–388.
[4] C.G.X. Wang, Research on wind environment for urban residential district in different building layouts [J], Build. Sci. 30 (7) (2014) 6–12.
[5] E. Ng, C. Yuan, L. Chen, et al., Improving the wind environment in high-density cities by understanding urban morphology and surface roughness: a study in Hong Kong [J], Landsc. Urban Plann. 101 (1) (2011) 59–74.
[6] B. Hong, B. Lin, Numerical studies of the outdoor wind environment and thermal comfort at pedestrian level in housing blocks with different building layout patterns and trees arrangement [J], Renew. Energy 73 (2015) 18–27.
[7] L. Chen, J. Hang, M. Sandberg, et al., The impacts of building height variations and building packing densities on flow adjustment and city breathability in idealized urban models [J], Build. Environ. 118 (2017) 344–361.
[8] J. Hang, Y. Li, M. Sandberg, et al., The influence of building height variability on pollutant dispersion and pedestrian ventilation in idealized high-rise urban areas [J], Build. Environ. 56 (2012) 346–360.

[9] T. Kubota, M. Miura, Y. Tominaga, et al., Wind tunnel tests on the relationship between building density and pedestrian-level wind velocity: development of guidelines for realizing acceptable wind environment in residential neighborhoods [J], Build. Environ. 43 (10) (2008) 1699–1708.
[10] American College of Laboratory Animal Medicine, Planning and Designing Research Animal Facilities [M], Academic Press, 2009, pp. 45–51.
[11] Di Li, Fang Li, Xin Huang, Yizong Lai, Shixiong Zheng, A model based integration framework for computer numerical control system development, Rob. Comp. Integ. Manuf. 26 (4) (2010) 333–343.
[12] Woowon Jeong, Jaehoon Seong, Comparison of effects on technical variances of computational fluid dynamics (CFD) software based on finite element and finite volume methods [J], Int. J. Mech. Sci. 78 (2014) 19–26.
[13] S. Murakami, Current status and future trends in computational wind engineering [J], J. Wind Eng. Ind. Aerod. 67&68 (1997) 3–34.
[14] B. Blocken, T. Stathopoulos, J.P.A.J. Van Beeck, Pedestrian-level wind conditions around buildings: review of wind-tunnel and CFD techniques and their accuracy for wind comfort assessment [J], Build. Environ. 100 (2016) 50–81.
[15] B. Blocken, J. Carmeliet, T. Stathopoulos, CFD evaluation of wind speed conditions in passages between parallel buildings—effect of wall-function roughness modifications for the atmospheric boundary layer flow [J], J. Wind Eng. Ind. Aerod. 95 (9–11) (2007) 941–962.
[16] C.W. Tsang, K.C.S. Kwok, P.A. Hitchcock, Wind tunnel study of pedestrian level wind environment around tall buildings: effects of building dimensions, separation and podium [J], Build. Environ. 49 (2012) 167–181.
[17] K.T. Tse, A.U. Weerasuriya, X. Zhang, et al., Effects of twisted wind flows on wind conditions in passages between buildings [J], J. Wind Eng. Ind. Aerod. 167 (2017) 87–100.
[18] J. Hang, Z. Luo, M. Sandberg, et al., Natural ventilation assessment in typical open and semi-open urban environments under various wind directions [J], Build. Environ. 70 (2013) 318–333.
[19] L. Tsichritzis, M. Nikolopoulou, The effect of building height and façade area ratio on pedestrian wind comfort of London [J], J. Wind Eng. Ind. Aerod. 191 (2019) 63–75.
[20] T. Ma, T. Chen, Classification and pedestrian-level wind environment assessment among Tianjin's residential area based on numerical simulation [J], Urban Clim. 34 (2020), 100702.
[21] O.S. Asfour, Prediction of wind environment in different grouping patterns of housing blocks [J], Energy Build. 42 (11) (2010) 2061–2069.
[22] T. Hu, R. Yoshie, Indices to evaluate ventilation efficiency in newly-built urban area at pedestrian level [J], J. Wind Eng. Ind. Aerod. 112 (2013) 39–51.
[23] L. Biao, J. Cunyan, W. Lu, et al., A parametric study of the effect of building layout on wind flow over an urban area [J], Build. Environ. 160 (2019), 106160.
[24] T. Shui, J. Liu, Q. Yuan, et al., Assessment of pedestrian-level wind conditions in severe cold regions of China [J], Build. Environ. 135 (2018) 53–67.
[25] M.A. Ancona, M. Bianchi, C. Biserni, F. Melino, S. Salvigni, P. Valdiserri, Optimum sizing of cogeneration plants by means of a genetic algorithm optimization: a case study [J], Case Stud. Therm. Eng. 15 (2019), 100525.
[26] Talha Orhan, Taşkın Kıvanç, Automated topology design of high-rise diagrid buildings by genetic algorithm optimization [J], Struct. Des. Tall Special Build. 30 (9) (2021) 1853.
[27] G. Mosetti, C. Poloni, B. Diviacco, Optimization of wind turbine positioning in large windfarms by means of a genetic algorithm [J], J. Wind Eng. Ind. Aerod. 51 (1) (1994) 105–116.
[28] S.A. Grady, M.Y. Hussaini, M.M. Abdullah, Placement of wind turbines using genetic algorithms [J], Renew. Energy 30 (2) (2005) 259–270.
[29] X. Ju, F. Liu, Wind farm layout optimization using self-informed genetic algorithm with information guided exploitation [J], Appl. Energy 248 (2019) 429–445.
[30] Y. Eroğlu, S.U. Se Kiner, Design of wind farm layout using ant colony algorithm [J], Renew. Energy 44 (2012) 53–62.
[31] M.A.E. Bilbao, Simulated annealing for optimization of wind farm annual profit [M], Int. Symp. Logist. Indust. Inform. (2009).
[32] J. Feng, W.Z. Shen, Design optimization of offshore wind farms with multiple types of wind turbines [J], Appl. Energy 205 (2017) 1283–1297.
[33] R. Archer, G. Nates, S. Donovan, et al., Wind turbine interference in a wind farm layout optimization mixed integer linear programming model [J], Wind Eng. 35 (2) (2011) 165–175.
[34] J. Park, K.H. Law, Layout optimization for maximizing wind farm power production using sequential convex programming [J], Appl. Energy 151 (2015) 320–334.
[35] O.A. Lo Brutto, S.S. Guillou, J. Thi Bot, et al., Assessing the effectiveness of a global optimum strategy within a tidal farm for power maximization [J], Appl. Energy 204 (2017) 653–666.
[36] S. Salcedo-Sanz, D. Gallo-Marazuela, A. Pastor-S Nchez, et al., Offshore wind farm design with the Coral Reefs Optimization algorithm [J], Renew. Energy 63 (2014) 109–115.
[37] D.Y. Ren Yanxiang, Application of Improved Genetic Algorithm in Maximum Utilization of Urban Land Space [M], in: Engineering Design and Computer Technology: the 15th National Engineering Design Computer Application Academic Conference, 2010. Harbin, China.
[38] W. Song, S. Dyke, Development of a cyber-physical experimental platform for real-time dynamic model updating [J], Mech. Syst. Signal Process. 37 (1–2) (2013) 388–402.
[39] A.-T. Nguyen, S. Reiter, P. Rigo, A review on simulation-based optimization methods applied to building performance analysis [J], Appl. Energy 113 (2014) 1043–1058.
[40] S. Khalili Araghi, R. Stouffs, Exploring cellular automata for high density residential building form generation [J], Autom. ConStruct. 49 (2015) 152–162.
[41] J. Zhang, P. Cui, H. Song, Impact of urban morphology on outdoor air temperature and microclimate optimization strategy base on Pareto optimality in Northeast China [J], Build. Environ. 180 (2020), 107035.
[42] Y. Du, C.M. Mak, Y. Li, Application of a multi-variable optimization method to determine lift-up design for optimum wind comfort [J], Build. Environ. 131 (2018) 242–254.
[43] X. Xu, Y. Liu, W. Wang, et al., Urban layout optimization based on genetic algorithm for microclimate performance in the cold region of China [J], Appl. Sci. 9 (22) (2019) 47.
[44] Le Cun, B. Boser, J.S. Denker, D. Henderson, R.E. Howard, W. Hubbard, L.D. Jackel, Backpropagation applied to handwritten zip code recognition [J], Neural Comput. 1 (1989) 541–551.
[45] H. Rowley, S. Baluja, T. Kanade, Neural Network-Based Face Detection [J], IEEE Computer Society, San Francisco, CA, USA, 1996, pp. 203–208.
[46] H. Rowley, S. Baluja, T. Kanade, Rotation Invariant Neural Network-Based Face Detection [J], IEEE Computer Society, Santa Barbara, CA, USA, 1998, pp. 38–44.
[47] S. Lawrence, C.L. Giles, Ah Chung Tsoi, Andrew D. Back, Face recognition: a convolutional neural-network approach [J], IEEE Trans. Neural Network. 8 (1) (1997) 98–113.
[48] P.Y. Simard, D. Steinkraus, J.C. Platt, Best Practices for Convolutional Neural Networks Applied to Visual Document Analysis [J], Seventh International Conference on Document Analysis and Recognition, 2003, pp. 958–963.
[49] Y. Lecun, L. Bottou, Gradient-based learning applied to document recognition[J], Proc. IEEE 86 (11) (1998) 2278–2324.
[50] J. Long, S. Evan, D. Trevor, Fully convolutional networks for semantic segmentation[J], IEEE Trans. Pattern Anal. Mach. Intell. 39 (4) (2015) 640–651.
[51] Junmo Koo, Gwon Deok Han, Hyung Jong Choi, Joon Hyung Shim, Wind-speed prediction and analysis based on geological and distance variables using an artificial neural network: a case study in South Korea [J], Energy 93 (2) (2015) 1296–1302.
[52] Afrasiabi Mousa, M. Mohammadi, Mohammad Rastegar, Shahabodin Afrasiabi, Advanced deep learning approach for probabilistic wind speed forecasting [J], IEEE Trans. Ind. Inf. (2020).
[53] Jinle Kang, Huimin Wang, Feifei Yuan, Zhiqiang Wang, Jing Huang, Qiu Tian, Prediction of precipitation based on recurrent neural networks in jingdezhen, jiangxi Province, China [J], Atmosphere 11 (3) (2020) 246.
[54] Manoj Verma, Harish Kumar Ghritlahre, Ghrithanchi Chandrakar, Wind Speed Prediction of Central Region of Chhattisgarh (India) Using Artificial Neural Network and Multiple Linear Regression Technique: A Comparative Study [J], Annals of Data Science, 2021 (pre-publish).
[55] Jianzhou Wang, Yining An, Zhiwu Li, Haiyan Lu, A novel combined forecasting model based on neural networks, deep learning approaches, and multi-objective optimization for short-term wind speed forecasting, Energy 251 (2022), 123960.

[56] DB 33/1092-2021) [S], Zhejiang Provincial Department of Housing and Urban and Rural Construction, the Design Standard for Green Building, 2021. Zhejiang, China.
[57] Ministry of Housing and Urban and Rural Construction of the People 's republic of china, Code for Fire Protection Design of Buildings (GB 50016-2014) [S], 2015. Beijing, China.
[58] Daily and annual data of China Meteorological Administration, China meteorological data. http://data.cma.cn, 2010.
[59] M.J. Soligo, P.A. Irwin, C.J. Williams, A comprehensive assessment of pedestrian comfort including thermal effects [J], J. Wind Eng. Ind. Aerod. (1998) 753–766.